Spinnability of Nanofilled Polypropylene

Denis Lorenzi,[1] *Gabriella Sartori,*[2] *Giuseppe Ferrara,*[2] *Luca Fambri**[1]

Summary: Spinnability of isotactic polypropylene iPP (melt flow 25 g/10 min) was studied after addition of three nanofillers at 0.3% by wt., two nanoclays and a modified hydrotalcite. TGA evidenced the increase of thermooxidation stability in nanofilled iPPs. All these iPP were successfully processed and tensile properties similar to those of iPP fibers were achieved. Processing and mechanical draw ratio were evaluated. Moreover, nanofilled iPP fibers appeared to be more prone to further drawing, as derived from both the maximum attainable strength and the maximum attainable drawing, as presented in the interpretation model of mechanical testing.

Keywords: drawing; fibers; nanofillers; polypropylene; processing

Introduction

Polypropylene fibers have many practical uses, like the production of carpets, furniture, packaging, construction and industrial materials, etc. Their thermal stability has attracted the attention of researchers, and various additive were proposed as flame retardant.[1] Various types of modified montmorillonite were studied in order to improve both processing and properties.[2] The effect of compatibilizing agent on nanofiller dispersion was properly remarked,[3] and various commercial and appositely synthesized products were added in percentage between 0.5 and 5% by wt. both in single or double step processing.[2–7] The molecular weight of iPP was properly considered in dependence on the nanofiller percentage and on the compatilizing agent; various melt flow grades iPP in the range of 2–3 dg/min,[4,6] 10–12 dg/min,[2,7–11] and at around 20–25 dg/min[11–14] were studied. Few literature data are available on nanofilled iPP fibers.[8–14]

This work will focus on the comparison of three different nanofillers for polypropylene fibers, two natural silicate nanolayers, and a synthetic hydrotalcite. The preparation procedure, and the coupling agent, PP-g-MA, to facilitate the nanofiller dispersion were selected according to the recent preparation of nanofilled iPP.[4] A special emphasis on the properties of the composites, their processability and the characteristics of the final fibers, in order to maintain the beneficial effects of the nanofiller.[1,6,13–15]

Experimental Part

Isotactic polypropylene iPP was a product of Lyondell-Basell Industries, Ferrara, Italy: melt flow index MFI (230 °C, 2.16 kg) = 25 ± 2 dg/min; density: 0.90 g/cm^3; crystallinity: 45%. Three different nanofillers were used: two organic modified cationic clays, Cloisite15A (Southern Clay Products) and Dellite 67G (Laviosa Chimica Mineraria), that are both montmorillonite ion-exchanged with octadecylammonium ions with the same amount of organic treatment; and Perkalite F100 (AkzoNobel) that is a synthetic hydrotalcite modified with a same amount of hydrogenated fatty acid. Polybond 3200 (Chemtura) was employed as coupling agent; it is a maleated PP (PP-g-MA) with 1.0% of grafted maleic anhydride and with a MFI (230 °C, 2.16 kg) of 115 dg/min.

[1] Department of Materials Engineering and Industrial Technologies, University of Trento, via Mesiano 77, 38123 Trento, Italy
E-mail: Luca.Fambri@ing.unitn.it
[2] Basell Poliolefine Italia srl of Lyondellbasell Industries, "G. Natta" R&D P.le L. Donegani 12, 44100 Ferrara, Italy

Table 1.
Melt flow and selected properties of iPP and nanofilled iPP.

	Nanofiller	Melt flow (dg/min) at 230 °C, 2.16 Kg	TGA Nitrogen Infl. Pt. (°C)	TGA Air Infl. Pt. (°C)	DSC 1st heating crystallinity (%)	DSC crystallization temperature (°C)	DSC 2nd heating crystallinity (%)
iPP	none	25	443	327	43	119	48
iPP-CLO	Cloisite	19	438	384	40	115	45
iPP-PER	Perkalite	22	442	350	39	123	45
iPP-DEL	Dellite	15	442	377	41	118	46

Thermostability of iPP and nanofilled iPP pellets was studied in thermogravimetric analysis by using a thermobalance Mettler TG50 both in air and in nitrogen flow of 200 ml/min with a heating rate 10 °C/min in the range 30–600 °C. The temperature of the maximum degradation rate was evaluated from the inflection point as evidenced from the peak derivative curve (see Table 1).

Differential scanning calorimetry (DSC) was performed on sample of about 15 mg by using a Mettler DSC 30 calorimeter, with a heating-cooling-heating cycle at ±10 °C/min in the range 0–250 °C flushing nitrogen at 100 ml/min. Melting temperature, ΔH_m, and melting enthalpy T_m were registered in the first and third scan, whereas crystallization temperature T_c and enthalpy ΔH_c were evaluated in the cooling step. The crystallinity content of the PP is calculated as $C = 100\ \Delta H_m/\Delta H_{mo}$, where $\Delta H_{mo} = 207$ J/g is the melting enthalpy of the crystalline phase of PP.[16] A slight decrease of crystallizability of nanofilled iPP was observed (see Table 1).

Mechanical properties of fibres were measured at room temperature by using an Instron tensile dynamometer mod. 4502 (cross-head speed of 10 mm/min, gage length of 20 mm) with thin paper test specimen mounting tab following ASTM D 3379.

Compounding

Nanofilled polymers were prepared by means of a double steps process. An initial masterbatch with 5% of nanofiller was produced with a single screw extruder by addition of PP-g-MA compatibilizer, as previously described.[4] Then, final iPP containing nanofiller at 0.3% by wt. was produced with a corotating and fully intermeshing twin screw Leistritz micro 27 extruder and eventually pelletized. Temperature of 180 °C along the screw and of 200 °C on the die were selected, whereas the melt presented a temperature of 196 °C. The velocity of the screw was of 200 rpm, with a cutter velocity of 25 m/min for the pellets cut. An appropriate filter was adjusted in the final part of the extrusion, in order to prevent any contamination and to avoid problems during the subsequent spinning of the fibers. Compounding extrusion was done putting special emphasize in the long residence time, in order to obtain a good dispersion of the master batch, and a controlled processing temperature, to protect the nanofiller from degradation. A lower melt flow index of the produced nanocomposites was found, as consequence of the mobility reduction after addition of nanofiller (Table 1), notwithstanding the high MFI of the compatibilizer. In particular, iPP-PER containing a synthetic hydrotalcite exhibited a MFI closer to pure iPP.

TGA analysis in nitrogen atmosphere showed no significant variation of thermograms. On the other hand, thermooxidation in air evidenced mass losses at higher temperature in the case of nanofilled iPP (see Table 1). In particular the onset of degradation peak from DTGA in Figure 1 was found at about 233 °C for pure iPP in

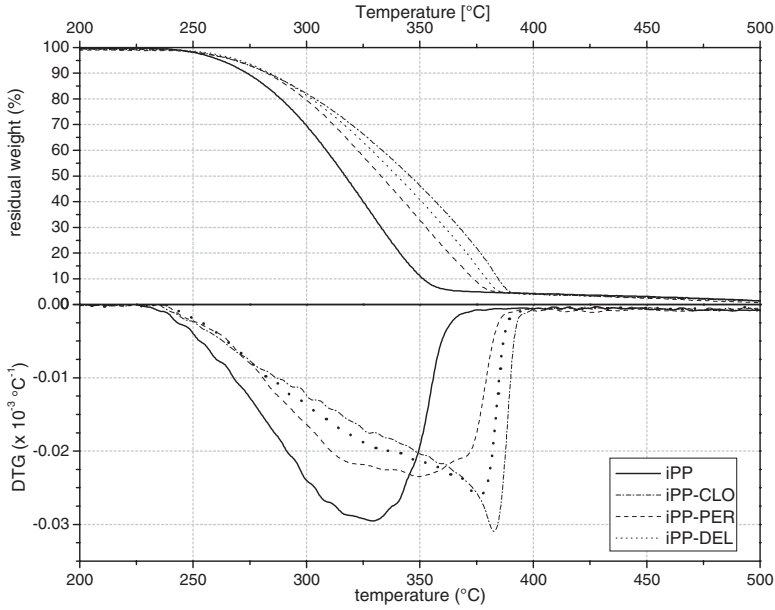

Figure 1.
TGA and DTGA thermograms of iPP and nano-filled iPP in air.

conformity to literature data [14] and about 237–239 °C in the case of nanofilled iPP. Moreover the effect of nanofiller on the rate of degradation of iPP in the range 250–300 °C resulted to decrease after addition of 0.3% of nanofiller (see the slope of DTGA curves). The maximum of degradation rate was found at 327 °C for iPP and at 350, 377 and 384 °C for iPP-PER, iPP-DEL and iPP-CLO respectively.

Crystallinity and crystallizability of nanofilled polymers were found lower (about 5–10%) than pure iPP, as revealed from the first and second heating in DSC analysis (Table 1 and Figure 2), in dependence on the 6% of master content. Moreover it should be noted a slightly higher melting temperature of iPP-PER, index of more perfect crystals, and a correspondent higher crystallization temperature in the cooling stage, suggesting a possible nucleating role of the modified hydrotalcite. The shoulder of the melting peak between 147 and 155 °C is related to low order crystals and it could be also attributed to the presence of hydrogenated fatty acids.

Fiber Spinning

Monofilaments were horizontally produced in a single step process (melt-extrusion and drawing) by using a lab-scale commercial extruder Estru 13 (Friulfiliere, Buia UD, Italy) with a single screw (D = 14 mm; L/D = 15; RC 2.5) with a single-hole spinnerette having diameter of 1.0 mm and capillary length/diameter ratio of 5, as previously described for polylactide fiber spinning.[17]

The effect of spinning was investigated with a constant screw rotation of 15 rpm with the same temperature profile of the cylinder between 180 and 200 °C, and die temperature of 200 °C. The collecting and drawing apparatus consisted in three rollers with a pulling drum (diameter of 200 mm) located at 70 cm and rotating between 25 and 250 rpm. Different spinning processes with controlled winding speeds at about 16, 32, 94 and 155 m/min were performed in order to produce fibers with modulated diameter and mechanical properties. Figure 3 shows the dependence of fiber diameter (D) on the winding speed (WS),

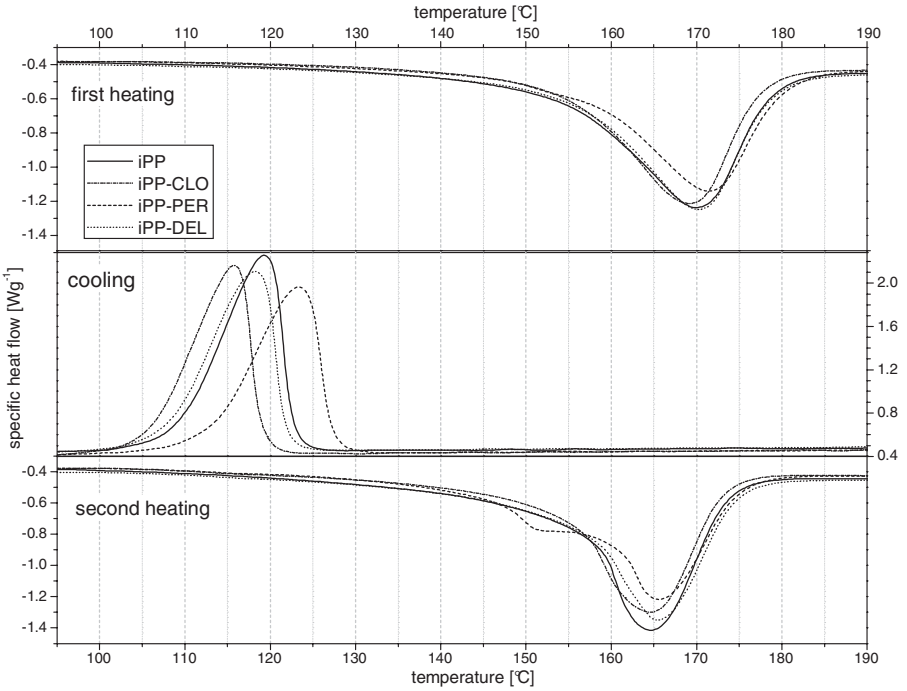

Figure 2.
DSC thermograms of iPP and nano-filled iPP in air (cycle at $\pm 10\ ^{\circ}C$/min).

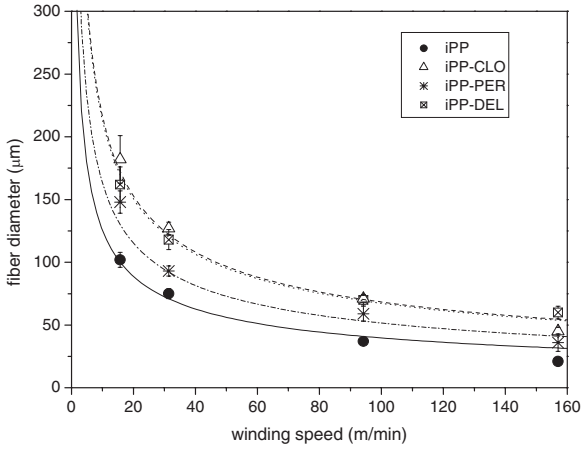

Figure 3.
Effect of winding speed on the diameter of representative iPP (●) and nano-filled iPP fibers. The lines represent the predicted value according to eq. (1) with $Q = 0.12\ cm^3$/min for iPP (continuous line). The dotted line refer to $Q = 0.21\ cm^3$/min (iPP-PER), $0.34\ cm^3$/min (iPP-CLO) and $0.37\ cm^3$/min (iPP-DEL) respectively.

considering the output Q of $0.12\ cm^3$/min for iPP and $0.21–0.37\ cm^3$/min for nano-filled iPP, following eq. (1)

$$D = 2 \times 1000\,(Q / (\pi WS))^{0.5} \qquad (1)$$

At low winding speed a certain effect of die-swelling could be observed, being the experimental diameter higher than that predicted from eq. (1). On the other hand above 100 m/min the diameter is lower than

expected due to the partial crystallinity of the fiber and the orientation of fibrils.

The corresponding velocity at the exit of the die of the various extrusions performed with the same temperature profile and the same screw rotation speed, was 0.1 m/min for iPP and 0.2–0.3 m/min for nanofilled iPP. It is also worth noting that in these conditions the output at 200 °C of nanofilled polymer and iPP resulted inversely proportional to their experimental melt flow at 230 °C. A combined effect of the nanofiller (0.3%) and of the PP-g-MA (5.7%) could properly affect the rheological behaviour of nanofilled iPP. The higher extrusion velocity of nanofilled iPP seem to be more effective than a higher swelling with respect to iPP, in order to interpret the higher fiber diameter during extrusion.

The effect of processing on fiber spinning can be properly described as a processing drawing, i.e. considering the section reduction with the increase of winding speed, as shown in Figure 4. In fact the processing draw ratio λ_{PRO} is defined as the ratio between the section of the die S_d and the section of the fiber S_f according to eq. (2)

$$\lambda_{PRO} = S_d/S_f = (D_d/D_f)^2 \quad (2)$$

where D_d and D_f are the diameter of the die and the fiber, respectively. It is well evident the progressive increase of draw ratio. For instance, fiber diameter between 180 and 20 microns can be obtained increasing λ_{PRO} in the range of 30–2300. The processing drawability (see Figure 4) decreases in the order iPP > iPP-PER > iPP-CLO > iPP-DEL, in the same direction of the melt flow reduction. Literature data refer an increase[13,14] or decrease [9] of nanofilled iPP melt flow.

Mechanical Evaluation

Stress at break of spun fibers was reported as function of strain at break in Figure 5. As expected the winding speed, the higher the strain at break and the lower the deformation at break for all the iPP composition. All data of both iPP and nanocomposite fibers appeared very similar. In particular deformation at break of nanofilled iPP resulted comparable or even higher than that of iPP. The apparent contrast to literature data where lower deformation at break of nanocomposites iPP fibers with respect to the initial iPP,[8,9,13,14] derived from the very low amount of nanofiller (0.3%) described in this paper and the

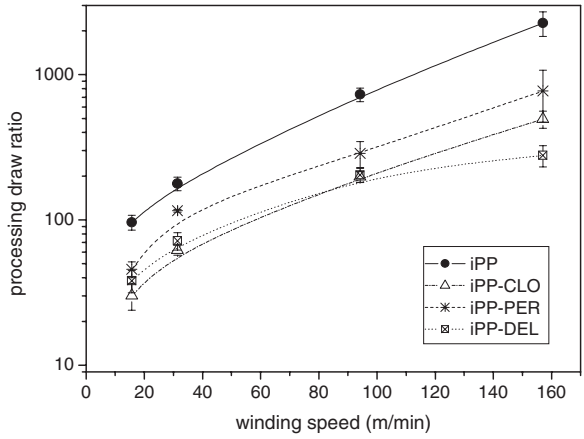

Figure 4.
Effect of winding speed on the processing draw ratio of selected iPP (●) and nano-filled iPP fibers, as evaluated according to eq. (2).

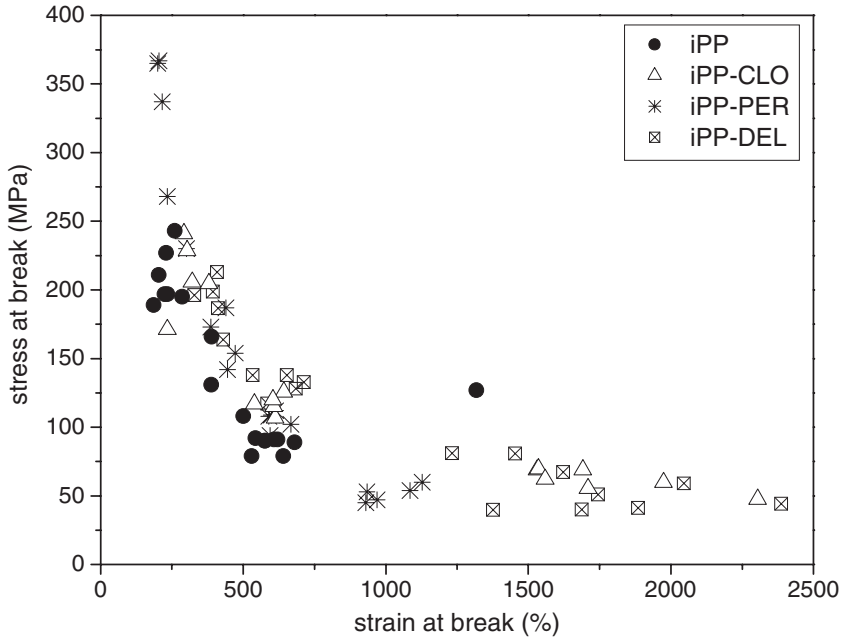

Figure 5.
Stress at break as function of strain at break of iPP and nanofilled iPP fibers.

higher content between 0.5 and 5% reported in literature.

Stress at break or tenacity was reported in many cases of literature [8,11–14] to increase after addition of 0.5–5% of nanofiller, even in the case of LLDPE as described by La Mantia et al. [18-19] In this latter case and in other papers [8,13,14] a higher modulus are also reported for nanofilled polyolefin, containing a much higher amount of nanofiller (1–5% by wt.) with respect to 0.3%. considered in this paper. It should be noted that even in literature the addition of nanofiller up to 1–5% in iPP determined in some cases a reduction of tenacity.[9,10,13,14]

The higher the winding speed, the lower the fiber diameter, the higher the drawing, the higher the orientation, and the higher the strength and the lower the deformation at break (see Figures). Moreover, the mechanical draw ratio λ_{PRO} [20] is defined according to eq. (3)

$$\lambda_{MEC} = (1 + \varepsilon_b/100) \quad (3)$$

where ε_b isthe strain at break. From these considerations, the maximum strength σ_{MAX}, can be evaluated from the effective stress at break σ_b and λ_{MEC}, taking into account the fiber section at the break, according to the equation (4)

$$\sigma_{MAX} = \sigma_b \lambda_{MEC} = \sigma_b (1 + \varepsilon_b/100). \quad (4)$$

Moreover, the total draw ratio, λ_{TOT}, depending on both processing and mechanical drawing, has been defined in eq. (5) combining eq. (2) and eq. (3)

$$\lambda_{TOT} = \lambda_{PRO} \times \lambda_{MEC}. \quad (5)$$

A more detailed evaluation can be obtained by the comparison of mechanical properties of selected fiber with average diameter of about 65 micron, as reported in Table 2. Stress at break in the range of 120 and 180 MPa and corresponding strain at break in between 150 and 625%, indicate a large differentiation of properties in dependence not only on the composition, but also on the processing. Following eq. (3),

Table 2.
Selected mechanical properties of iPP and nanofilled iPP fibers of analogous diameter.

	Fiber diameter (micron)	Linear density (tex)*	Processing draw ratio λ_{PRO}	Stress at break (MPa)	Deformation at break (%)	Mechanical draw ratio λ_{MEC}	Maximum strength – Tenacity* (MPa-cN/tex)	Total draw ratio λ_{TOT}
iPP	64 ± 4	2.9 ± 0.4	244	176 ± 35	317 ± 89	4.2	734 - 81	1018
iPP-CLO	68 ± 1	3.3 ± 0.1	216	123 ± 4	624 ± 27	7.2	891 - 99	1566
iPP-PER	66 ± 2	3.1 ± 0.2	230	136 ± 22	510 ± 91	6.1	830 - 92	1400
iPP-DEL	63 ± 4	2.8 ± 0.4	252	178 ± 34	442 ± 64	5.4	965 - 107	1366

*for definition of Linear density and Tenacity see ASTM.[21]

mechanical draw ratio of nanofilled iPPs is higher than iPP.

From these data, in the case of nanofilled iPPs it is evident a higher maximum strength or from eq. (4), and a higher maximum drawability or total draw ratio from eq. (5) with respect to iPP. In particular maximum strength between 830–965 MPa, and total draw ratio of about 1350–1550 for nanofilled iPP fibers, in comparison to 734 MPa and 1018 of iPP fibers respectively. Following experimental processing, these formulations of nanofilled polypropylene can be easily spun, resulting in analogous mechanical properties to those of the pristine polypropylene. However, notwithstanding similar processing draw ratio of about 220–250 were measured, much higher mechanical draw ratio (about 5–7 vs. 4) and hence total draw ratio (about 1300–1500 vs. 1000) were evaluated in the case of nanofilled iPPs vs. pure iPP. Moreover, according to extrapolated data of maximum attainable draw ratio and strength, the addition of Cloisite or Dellite or Perkalite to the formulation appeared positive in polypropylene processing and in the properties of the resulting spun fibers, promoting the ductility of the materials, diminishing the needed load and rising the maximum elongation before the break. Furthermore, from the diameter ratio of all tensile test before and after the break, an interesting evaluation of drawability of iPP fiber can be obtained. Figure 6 shows the dependence of diameter at break on the initial diameter for iPP and various nanofilled iPP. The lower the slope of the best fit line $Y = B^*X$, the higher the drawability of the material. In particular

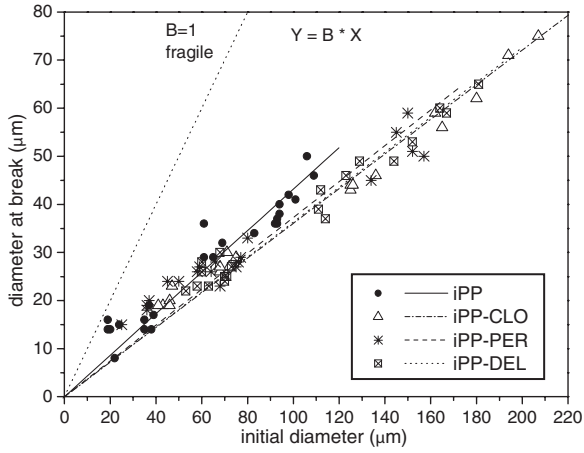

Figure 6.
Diameter at break as function of the initial diameter of iPP and nanofilled iPP fibers.

the slope decreases from iPP to nanofilled-iPPs in the order iPP(0.43 ± 0.01) >> iPP-PER(0.37 ± 0.01) > iPP-DEL(0.363 ± 0.006) > iPP-CLO (0.360 ± 0.006).

Moreover, considering the inversion of x-y axes of Figure 6, the slope of the best fit line 1/B of the new plot (not reported) is related to the mechanical draw ratio (λ_{MEC}), according to the eq. $\lambda_{MEC} = 1/B^2$.

It is possible to evaluate an overall mechanical draw ratio as average result of all fibers reported in Figure 6 and having diameter in the range of about 20–200 micron, and it increases as follows

$$\text{iPP}\,(5.2 \pm 0.6) << \text{iPP-PER}\,(6.9 \pm 1.1) < \text{iPP-DEL}\,(7.5 \pm 0.6) \leq \text{iPP-CLO}\,(7.6 \pm 0.6)$$

These overall mechanical draw ratios resulted slightly higher, than those reported in Table 2.

TEM pictures of a transversal cut on a nanofilled iPP-CLO fiber are shown in Figures 7A and 7B. They are representative of the other nanofilled iPP fibers and they are sufficient to explain all the benefits described for the fibers obtained with these nanocomposites. In fact, the clay layers have been well separated forming small tactoids homogeneously dispersed inside the fibres. Figure 7A shows an homogeneous distribution of nanofiller in iPP matrix; whereas tactoids having about length of 100 nm and thickness of 20–50 nm, are well represented in Figure 7B.

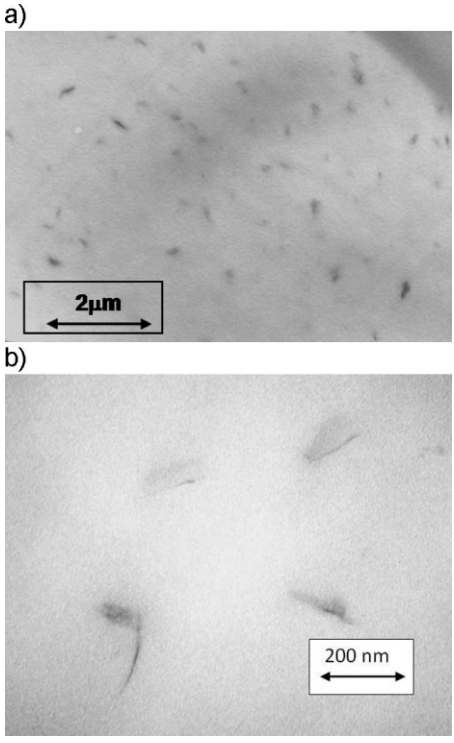

Figure 7.
A) Standard magnificationTEM picture of a transversal cut on a nanofilled iPP fiber. B) High magnification TEM picture of a transversal cut on a nanofilled iPP fiber.

Conclusion

In conclusion, three type of nanocomposite iPPs at low content of 0.3% nanofiller were properly prepared for fiber production. TGA revealed during thermooxidation the beneficial effect of all nanofillers on mass loss retardation by increasing both the onset temperature and the temperature of the maximum degradation rate. The introduction of modified hydrotalcite with hydrogenated fatty acids evidenced a somewhat effect of nucleation of iPP.

All nanofilled iPPs in these specific processing conditions could be easily spun, with resulting fibers comparable to those of iPP, even if a lower processing draw ratio could be reached as consequence of the lower melt flow of the compounded iPPs. However, a larger ductility was found for nanofilled iPP fibers, and selected fibers with diameter of about 65 micron (3tex) evidenced deformation at break about 40–100% higher than those of pure iPP.

The clay layers have been well separated and homogeneously dispersed inside the fibres, and appeared to be responsible of the higher ductility of the nanofilled iPP materials.

After evaluation of both the processing draw ratio and the mechanical draw ratio, a total draw ratio has been derived, from

whom the nanofilled iPPs appeared more prone to a higher drawing than iPP. By simple spinning and drawing at various collecting rates, and consequent mechanical testing of the produced fibers, the maximum attainable strength and the maximum attainable draw ratio could be evaluated for the selected polymers. All the nanofilled iPPs with respect to the pristine iPP showed not only a higher maximum of strength (about 800–1000 MPa vs. 700 MPa) or tenacity (about 90–110 cN/tex vs. 80 cN/tex), but also a higher maximum drawability (about 1300–1500 vs 1000). These results can be properly used for further planning and optimisation of nanocomposite fiber processing conditions.

[1] S. Zhang, A. R. Horrocks, *Prog. Polym. Sci.* **2003**, *28*, 1517.
[2] D. Garcìa-Lòpez, O. Picazo, J. C. Merino, J. M. Pastor, *Eur.Pol.J.*, **2003**, *39*, 945.
[3] S. G. Lei, S. V. Hoa, M.-T. Ton-That, *Comp. Sci. Techn.*, **2006**, *66*, 1274.
[4] E. M. Benetti, V. Causin, C. Marega, A. Marigo, G. Ferrara, A. Ferraro, M. Consalvi, F. Fantinel, *Polymer*, **2005**, *46*, 8275.
[5] J. Li, M.-T. Ton-That, S.-J. Tsai, *Pol. Eng. Sci.*, **2006**, *46*, 1060.
[6] J. Golebieswski, A. Galeski, *Comp. Sci. Techn.*, **2007**, *67*, 3442.
[7] J. Li, M.-T. Ton-That, W. Leelapornpisit, L. A. Utracki, *Pol. Eng. Sci.*, **2007**, *47*, 1447.
[8] M. Joshi, M. Shaw, B. S. Butola, *Fibers and polymer*, **2004**, *5*, 59.
[9] S. H. Lee, J. R. Youn, *J. Appl. Polym. Sci.* **2008**, *109*, 1221.
[10] M. S. Smole, K. Stakne, K. S. Kleinschek, M. Kurecic, M. Bele, D. G. Svetec, V. Ribitsch, *J. Appl. Pol. Sci.*, **2009**, *113*, 1276.
[11] A. Marcincin, M. Hricova, K. Marcincin, A. Hoferikova, J. Legen, *Fibres & Textile.* **2007**, *15*(5–6), 64.
[12] Z. Mlynarcikova, E. Borsig, J. Legen, A. Marcincin, P. Alexy, *J. Macromol. Sci., A Pure Appl. Chem.* **2005**, *42*, 543.
[13] A. R. Horrocks, B. K. Kandola, G. Smart, S. Zhang, T. R. Hull, *J. Appl. Polym. Sci.* **2007**, *106*, 1707.
[14] G. Smart, B. K. Kandola, A. R. Horrocks, S. Nazaré, D. Marney, *Polym. Adv. Technol.* **2008**, *19*, 658.
[15] S. Zhang, T. R. Hull, A. R. Horrocks, G. Smart, B. K. Kandola, J. Ebdon, P. Joesph, B. Hunt, *Pol. Degr. Stab.*, **2007**, *92*, 727.
[16] D. W. Van Krevelen, "*Properties of Polymers*", 3rd Ed. Elsevier, Amsterdam **1990**, p. 121.
[17] L. Fambri, S. Bragagna, C. Migliaresi, *Macromol.-Symp.*, **2006**, *234*, 20.
[18] F. P. La Mantia, N. Tzankova Dintcheva, R. Scaffaro, R. Marino, *Macr. Mat. Eng.*, **2008**, *293*, 83.
[19] N. Tzankova Dintcheva, R. Marino, F. P. La Mantia, *e-Polymers*, **2009**, n.054.
[20] J. George Tomka, in: "*Comprehensive Polymer Science*" vol. 2, In: C., Booth, C. Price, Eds., Pergamon Press, Oxford **1989**, p. 506.
[21] ASTM D 126-09 "Standard terminology Relating to Textile".

